PAPER

Modulating the porosity of activated carbons *via* pre-mixed precursors for simultaneously enhanced gravimetric and volumetric methane uptake†

Afnan Altwala[ab] and Robert Mokaya [ID] *[a]

Pre-mixed precursors containing biomass-derived carbonaceous matter of varying O/C ratio and polypyrrole have been used as starting materials to modulate the porosity of activated carbons. The use of pre-mixtures of polypyrrole and CNL carbon (from accidental and uncontrolled burning of wood under fierce fire conditions of the first Carbon Neutral Laboratory, CNL, building at Nottingham) or polypyrrole and ACDS carbon (air-carbonised date seed) generates activated carbons with substantially greater surface area than single use of any of the precursors. Mixing of CNL carbon or ACDS carbon, which are known to generate highly microporous carbons, with polypyrrole, which generates mesoporous carbons, yielded activated carbons with a much wider range of porosity. More importantly, it is possible to prepare activated carbon with ultra-high surface area (up to 3890 m^2 g^{-1}) and pore volume (up to 2.40 cm^3 g^{-1}) in a manner not possible *via* single use of any of the precursors. The resulting ultra-high surface area carbons have excellent gravimetric methane uptake, which at 25 °C and 100 bar, can reach up to 28.4 mmol g^{-1} (or 0.46 g g^{-1}). In addition to the excellent gravimetric uptake, at 25 °C and 100 bar, the carbons have total volumetric methane uptake of up to 260 cm^{-3} (STP) cm^{-3}, and working capacity (100–5 bar) of 210 cm^{-3} (STP) cm^{-3}. The combination achieved for gravimetric and volumetric uptake is higher and more attractive than any previous value for porous carbons or metal–organic-frameworks (MOFs).

1. Introduction

Currently, the world is facing enormous challenges as a result of rising greenhouse gas emissions, which are causing severe global warming concerns. A number of potential solutions are the focus of on-going research, which is targeted towards the remediation of environmental damage emanating from CO_2 release especially from fossil fuel power stations.[1–3] As a consequence of increasing climate change concerns and the tightening of environmental regulations, natural gas, of which the main component is methane, has recently attracted attention as a less environmentally damaging fuel.[4–10] On the other hand, biogas, which is produced from the breakdown of organic matter and largely consists of methane, has also attracted interest as a renewable fuel source.[11,12] Biogas and natural gas, both of which consist of over 70% methane, are readily available

and pose a lower environmental risk when used as fuel; although CO_2 is produced, biogas or natural gas burn more cleanly than petroleum-based fuels.

The main obstacles to the more widespread use of methane-rich gases as fuels is to do with their lower energy density and challenges associated with their storage and transportation when compared to gasoline and diesel. Natural gas may be stored in compressed form as compressed natural gas (CNG) or in liquid form as liquefied natural gas (LNG). However, both CNG and LNG are not ideal as they cannot operate under ambient temperature and pressure; while CNG needs high pressure (typically 200–300 bar) conditions requiring expensive holding vessels, LNG is dependent on expensive cryogenic cooling techniques.[13] A promising method that may overcome the pressure and temperature concerns regarding methane storage is the use of adsorbed natural gas (ANG). Storage of adsorbed methane, typically involving physisorption onto the surface of porous adsorbents, can operate at low pressure conditions and at ambient temperature, both of which can reduce costs and offer improved ease of usage.[4–10,14,15] Porous carbons are amongst the materials currently being explored for the storage of methane.[4–10] Porous carbons, and specifically activated carbons, have a number of attractive characteristics including controllable porosity, low cost, chemical and mechanical stability, and ease of preparation and handling.[16,17]

[a]School of Chemistry, University of Nottingham, University Park, Nottingham NG7 2RD, UK

[b]Department of Chemistry, College of Science Al-Zulfi, Majmaah University, Al-Majmaah, 11952, Saudi Arabia. E-mail: r.mokaya@nottingham.ac.uk

† Electronic supplementary information (ESI) available: Ten additional figures; TGA curves, XRD patterns, SEM and TEM images, nitrogen sorption isotherms and pore size distribution curves, comparative gravimetric and volumetric methane uptake isotherms, and six tables; comparative elemental, textural and methane uptake. See https://doi.org/10.1039/d2ta00421f

13744 | *J. Mater. Chem. A*, 2022, **10**, 13744–13757

This journal is © The Royal Society of Chemistry 2022

The nature and type of carbonaceous precursor utilised, as well as the activation process and conditions, influence the properties of activated carbons.

The main focus of this study was the judicious use of pre-mixed precursors to synthesis activated carbons that are suited for enhanced methane storage. The pre-mixed precursors, which contain materials that are known to respond variably to similar levels of activation, are used a means to modulate the porosity of activated carbons in a targeted manner. Our improved understanding of the way in which the activation process for biomass is influenced by the carbonisation phase is combined with the known effects of the oxygen/carbon (O/C) ratio of the precursors used in order to provide activated carbons with optimum porosity and high packing density that are ideal for methane storage.[18–22] We have recently shown that the nature of a carbonaceous precursor has significant influence on susceptibility to activation and, consequently, plays a key role in determining the balance between microporosity and mesoporosity in the resulting carbons.[23–28] Some biomass-derived carbonaceous matter, depending on the type of biomass and method of carbonisation, can be highly resistant to activation and therefore tend to yield activated carbons with significant microporosity.[18,20,22,24] In particular, air-carbonisation of biomass yields carbonaceous matter with relative low oxygen content (*i.e.*, low O/C ratio), which is resistant to activation.[18,20,22] Such resistance to activation results in highly microporous activated carbons that have high packing density but with surface area that hardly goes above 2800 m^2 g^{-1}.[18,20,22] When used for gas uptake, such carbons have low gravimetric uptake (due to limited surface area) but comparatively high volumetric uptake (due to high packing density).[22] On the other hand, polypyrrole is readily activateable and can yield highly mesoporous activated carbons that have much higher surface area of up to 4000 m^2 g^{-1}, but also have large pore volume and low packing density.[21,29–34] This translates to high gravimetric gas uptake but comparatively low volumetric capacity.[33] However, blending the polypyrrole with low value waste biomass-derived carbonaceous matter can achieve pre-mixed precursors that may still generate activated carbons with ultra-high surface area but which also have higher packing density. This would enable synthesis of activated carbons that have optimised properties (with respect to surface area and packing density) for which both the gravimetric and volumetric gas uptake is high in a manner not possible for single use of either the polypyrrole or biomass-derive carbonaceous matter.

We have previously explored the preparation of activated carbons from pre-mixed precursors that contain a mixture of precursors that respond variably to similar levels of activation.[21] Polypyrrole was mixed with raw eucalyptus wood sawdust (O/C ratio of 0.773) or hydrochar (O/C ratio of 0.483) derived from the sawdust following hydrothermal carbonisation.[21] On the other hand, this study explores the use of pre-mix precursors made up of polypyrrole and biomass-derived carbonaceous matter with much lower oxygen content (*i.e.*, very low O/C ratio), namely, air carbonised date seed (O/C ratio of 0.156)[22] and so-called CNL carbon (O/C ratio of 0.185).[18,22] The overall aim of the study is to demonstrate that a logical process can be used to make activated carbons with appropriate porosity and packing density that enables record methane storage capacity.

In order to enable widespread use of methane, the Advanced Research Projects Agency-Energy (ARPA-E) of the U.S. Department of Energy (DOE) has recently set a volumetric storage capacity target of 350 cm^3 (STP) cm^{-3} and gravimetric storage capacity of 0.5 g (CH$_4$) g^{-1} at room temperature and pressure of 35 to 100 bar. It is important to note that the target of 350 cm^3 (STP) cm^{-3} was set at that level to take into account the use of the crystallographic density of MOFs in calculating volumetric uptake.[5,7] Given that the crystallographic density of MOFs is typically at least 25% higher than their actual packing density, the target of 350 cm^3 (STP) cm^{-3} incorporates an expected reduction of at least 25% (down to *ca.* 263 cm^3 (STP) cm^{-3}) once MOFs are packed into storage tanks. Crucially, this reduction does not apply to activated carbons for which volumetric uptake is usually calculated using experimentally determined packing density. In this regard, the target for methane storage in carbons can be considered to be 263 cm^3 (STP) cm^{-3}. This study was motivated by the fact that the key to achieving high methane storage capacity in porous materials, both in terms of gravimetric and volumetric capacity, is related to having adsorbents with a good balance between surface area and packing density. This study, therefore, exploits the fact that to present both high surface area and packing density, an adsorbent's porosity should arise predominantly from micropores, but accompanied by the presence of a significant proportion of small mesopores.[4–9]

2. Experimental section

2.1 Material preparation

The date seed (5 g) was placed in an alumina boat and heated in a horizontal tube furnace to 400 °C under an atmosphere of nitrogen at heating ramp rate of 10 °C min^{-1}. Once at 400 °C, the date seed was exposed to a flow of air only for 5–10 minutes, after which the furnace was left to cool under a flow of nitrogen gas only. The resulting carbonaceous matter was designated as ACDS (*i.e.*, air carbonized date seed) carbon. CNL carbon, from the surface of a burnt wood log, was washed with distilled water to remove any impurities, dried in an oven at 120 °C overnight and sieved to obtain a homogenous particle size of ∼212 mm. Polypyrrole (designated as PPY) was prepared by adding 3 g of pyrrole to 200 mL of 0.5 M FeCl$_3$ solution and stirring the mixture for 2 h at room temperature. The polypyrrole was recovered, washed with distilled water and dried in an oven at 120 °C. The yield from pyrrole to polypyrrole was close to 100%. For activation, two sets of samples were prepared from mixtures of PPY/CNL or PPY/ACDS. Mixtures of PPY : CNL : KOH or PPY : ACDS : KOH at weight ratio of 1 : 2 : 4, 1 : 1 : 4 or 2 : 1 : 4 were activated at 800 °C. The amount of KOH and activation temperature (800 °C) were identical for all preparations. The mixtures were ground until homogeneous and placed in a tube furnace and heated under nitrogen for 1 h at 800 °C following a heating ramp rate of 3 °C min^{-1}. After cooling, the activated carbons were thoroughly washed with 10 wt% HCl, followed by washing with distilled water until neutral pH was achieved for the filtrate. The activated

This journal is © The Royal Society of Chemistry 2022

J. Mater. Chem. A, 2022, **10**, 13744–13757 | **13745**

carbons were dried overnight in an oven at 120 °C. Single source carbons were designated as PPYx*T*, CNLx*T* and ACDSx*T*, where x is the KOH/precursor ratio (*i.e.*, 4) and *T* is activation temperature (800 °C). Carbons from pre-mixed precursors were designated as PPYCNLxyz or PPYDSxyz where xyz is ratio (x : y : z) of the x = PPY, y = CNL or ACDS, and z = KOH.

2.2 Material characterisation

Thermogravimetric analysis (TGA) was performed using a TA Instruments Discovery analyser or TA Instruments SDT Q600 analyser under flowing air conditions (100 mL min^{-1}). A PANalytical X'Pert PRO diffractometer was used to perform powder XRD analysis using a Cu-Kα light source (40 kV, 40 mA) with step size of 0.02° and 50 s time step. Elemental, CHN, analysis was performed on an Exeter Analytical CE-440 Elemental Analyser. Nitrogen sorption analysis (at −196 °C), with a Micromeritics 3FLEX sorptometer, was used for porosity assessment and for determination of textural properties. Prior to analysis the carbon samples were degassed under vacuum at 200 °C for 12 h. Surface area was calculated using the Brunauer–Emmett–Teller (BET) method applied to adsorption data in the relative pressure (P/P_0) range of 0.02–0.22. The relative pressure range was selected to ensure a positive *y*-axis intercept from multipoint BET fitting (such that $C > 0$) and that $V_{ads}(1 − P/P_0)$ would increase with P/P_0.[35] The pore volume was estimated from the total nitrogen uptake at close to saturation pressure ($P/P_0 \approx$ 0.99). The micropore surface area and micropore volume were determined *via* t-plot analysis. The pore size distribution (PSD) for each carbon was determined using Non-local density functional theory (NL-DFT) applied to nitrogen adsorption data. PSDs were determined using SAIEUS software with the 2D-NLDFT heterogeneous surface kernel, which allowed the calculations to adequately take account of the chemical and energetic heterogeneity of the carbons. The fitting parameter, λ, within the SAIEUS software, which controls the roughness of the PSD, was selected to be between 2.5 and 5.0 so as to generate the most realistic PSD for carbons.[36,37] Scanning electron microscopy (SEM) images were recorded using an FEI Quanta 200 microscope operating at a 5 kV accelerating voltage. Transmission electron microscopy (TEM) images were obtained using a JEOL 2100F instrument operating at 200 kV and equipped with a Gatan Orius CCD for imaging. Prior to analysis, the carbon samples were suspended in distilled water and dispersed onto lacey carbon support films.

2.3 Methane uptake measurements

Methane uptake was determined using a Hiden Isochema XEMIS Analyser. Before the uptake measurements, the carbon samples were degassed at 240 °C under vacuum for several hours. Methane uptake isotherms were obtained at 25 °C over the pressure range of 0 to 100 bar. To determine isosteric heat of adsorption (Q_{st}), experimental isotherms were fit to a Toth model using pyGAPS modelling module. The returned parameters (n_m, K, m) of the model were then used to calculate Q_{st} according to the Whittaker method.

3. Results and discussion

3.1 Yield, nature and elemental composition of activated carbons

When preparing activated carbon, choosing the right starting materials is essential in order to generate the targeted porosity. Pre-mixed precursors were employed, with the hope that they would offer superior potential for porosity generation compared to single precursors. A further important consideration is the elemental analysis of the starting materials and in particular their O/C atomic ratio. Based on previous studies,[22] date seed (*Phoenix dactylifera*) was chosen as a starting material due to its low elemental oxygen content. Additionally, and for completeness, CNL carbon was chosen as the other biomass source since it also exhibits a low O/C atomic ratio. When compared with a variety of biomass sources, the elemental composition of the biomass-derived precursors employed in this study were found to have comparatively low O/C atomic ratios, *i.e.*, 0.185 and 0.156 for CNL carbon and ACDS carbon, respectively. These are the lowest oxygen contents across a wide range of biomass sources for which the O/C ratio is typically in the range of 0.77 to 1.0 (ESI Table S1†).

The next consideration was selection of flash air-carbonisation as the method for converting the raw date seed into carbonaceous matter that would then be activated. This would not only negate the requirement for hydrothermal carbonisation (HTC) or pyrolysis but also achieve carbonaceous material with the lowest O/C ratio. Although both HTC and air-carbonisation diminish the O/C ratio compared to raw biomass, previous studies have demonstrated that the latter causes a bigger decrease.[18,20,22] For example, when eucalyptus sawdust is exposed to HTC, the O/C ratio reduces from 0.773 to 0.484 (a 40% reduction), while air carbonisation lowers the O/C ratio to 0.251 (*ca.* 70% decrease).[20] In addition, the CNL carbon chosen as precursor was sourced from the charred remains of the accidental and uncontrolled burning of wood under fierce fire conditions in the School of Chemistry's first CNL building.[18]

Table 1 Elemental composition of precursors (polypyrrole, CNL carbon and ACDS carbon) and activated carbons derived from single precursors or pre-mixed precursors

Sample	Yield [wt%]	C%	H%	N%	O%	O/C^a
PPY		55.5	2.7	16.0		
PPY4800	12	89.0	0.1	0.7	10.2	0.084
CNL		77.7	3.1	0	19.2	0.185
CNL4800	32	84.2	0.0	0.0	15.8	0.141
PPYCNL124	30	83.0	0.0	0.0	17.0	0.154
PPYCNL114	20	91.0	0.0	0.0	9.0	0.074
PPYCNL214	20	91.0	0.0	0.0	9.0	0.074
Raw DS		49.0	7.0	1.6	42.4	0.649
ACDS		78.5	4.0	2.1	16.3	0.156
ACDS4800	50	84.3	0.1	0.1	15.5	0.138
PPYDS124	36	85.0	0.2	0.4	14.4	0.127
PPYDS114	22	90.5	0.2	0.2	9.1	0.075
PPYDS214	20	90.0	0.0	0.0	10.0	0.083

^{a} Atomic ratio.

13746 | *J. Mater. Chem. A*, 2022, **10**, 13744–13757

This journal is © The Royal Society of Chemistry 2022

Thus, both the ACDS and CNL carbons were obtained *via* air carbonisation of, respectively, wood or date seeds.

The yields of the activated carbons are shown in Table 1. The yields are related to the ease of activation of the precursor. PPY is the least resistant to activation and accordingly sample PPY4800 has the lowest yield of 12 wt%. The yields of CNL4800 and ACSD4800 are, respectively 32 and 50 wt%, which is in line with the trend in their O/C ratios. For both series of samples, the yields from pre-mixed precursors are lower than for the single use of biomass precursor and reduce as the amount of PPY in the mixture increases. At any given pre-mixture level, the PPY/ACDS mixtures have higher yield, which again is consistent with the fact that the ACDS carbon has a lower O/C ratio compared to CNL carbon.

The elemental composition of the precursors, *i.e.* PPY, ACSD carbon and CNL carbon, and the activated carbons are shown in Table 1. The C content of the activated carbons increases compared to that of the precursors, which is accompanied by a decrease in N, H and O. The carbon content of PPY increases from 55.5 to 89 wt% when it is activated (sample PPY4800), whereas the N and H contents decrease from 16.0 and 2.7 to 0.7 and 0.1 wt%, respectively. On activation of the CNL carbon (sample CNL4800), the C content increases from 77.1 to 84.2 wt% and the H (1.0 wt%) and N (2.9 wt%) fractions are virtually removed. When ACDS carbon is subjected to activation (sample ACDS4800), the carbon content rises from 78.5 to 84.3 wt% along with a decrease in the N and H component from 2.1 and 4.0, respectively to 0.1 wt%. All the activated carbons, regardless of the precursor, have a C content of between 78.5 and 91 wt%. It can be surmised from the elemental composition data (Table 1) that the activated carbons have comparable C and O contents regardless of the form of pre-mixed precursor from which they are derived. Furthermore, the N and H content of both sets of samples remains low, and becomes practically nil in samples made from pre-mixed precursors containing a high quantity of PPY or CNL.

To further probe their nature, the carbons were thermally treated to 800 °C at a rate of 10 °C min^{-1} under flowing air conditions. TGA was performed in order to determine the purity of the carbons, *i.e.*, absence of inorganic matter, as well as their thermal stability. The TGA curves (ESI Fig. S1†) show that the carbons are stable up to 450 °C following an initial mass loss of 2–5 wt% below 300 °C, which is due to the loss of water or volatiles. This is followed by the main mass loss event due to carbon burn-off at temperatures ranging from 450 to 620 °C. The carbons burn-off within a similar temperature range, which indicates that they have comparable thermal stability. This is a consequence of the fact that they were all activated at 800 °C. All the carbons have a residual mass of less than 2%, and most have no residual mass indicating that they are fully carbonaceous with only trace or nil amounts of inorganic matter.

Powder XRD is useful in determining the nature (with respect to graphitisation) of carbons and also for confirming the absence of any crystalline inorganic phases that would show sharp peaks. The XRD patterns of the precursors (ESI Fig. S2†) are featureless except for weak and broad peaks at 2-theta of 22° and 44°, which may be ascribed to very limited graphene

stacking. The XRD patterns of the activated carbons (ESI Fig. S2†) hardly show the peaks due to graphene stacking, which is consistent with the expectation that activation would disrupt any graphitic domains. It is clear from the XRD patterns that the carbons generated from pre-mixed precursors are largely amorphous, as is characteristic of KOH-activated carbons. Given the heterogeneous nature of the starting carbonaceous matter, it is interesting to observe that the activated carbons are homogeneous (one-phase) materials.

Scanning electron microscopy was used to examine the surface structure and morphology of the activated carbons. Polypyrrole is known to have globular morphology with globular and spherical particles loosely grouped into bigger assemblies,[38] while both CNL carbon and ACDS carbon have previously been shown to retain, respectively, the woody or extended honeycomb structure of their respective biomass sources.[18,20,22] The SEM images of representative activated carbons (ESI Fig. S3†) indicate that, regardless of the composition of the pre-mixed precursor, the resulting activated carbons have a particle shape that is drastically different from the precursors. The activated carbons comprise of smooth-surfaced particles with extensive conchoidal cavities. This particle morphology is similar to that observed in activated carbons produced from a variety of sources.[16,18–25,34] This is consistent with the fact that it is now well-recognised that all activated carbons produced by KOH activation have a similar appearance, and that the type of precursor material has little effect on the morphology. The TEM images of the activated carbons (ESI Fig. S4†) demonstrate wormhole-type pore channels and hierarchical porosity with no indication of graphitic domains which is consistent with the XRD patterns and previous research on biomass-derived activated carbons.[18–27]

3.2 Textural properties and porosity

The nitrogen sorption isotherms and corresponding pore size distribution (PSD) curves for the PPY/CNL set of samples, and the PPY-only derived sample (PPY4800) and the CNL-only derived sample (CNL4800) are shown in Fig. 1. It is worth noting that the PPY-only derived sample (PPY4800) displays an isotherm that is typical of a primarily mesoporous material, whilst the isotherm for the CNL-only derived sample (CNL4800) indicates the presence of a significant proportion of micropores and supermicropores with only a small proportion of small mesopores.[18,20,22,31–34] The isotherms of the PPY/CNL activated carbons show some clear trend with respect to the nature of the pre-mix precursors. Firstly, the total amount of nitrogen adsorbed, which is an indication of the overall porosity generated, increases as the amount of PPY in the pre-mixture rises in the order CNL4800 < PPYCNL124 < PPYCNL114 < PPYCNL214. Secondly, the shape of the isotherms gradually change with the proportion of PPY. The isotherm of CNL4800 is type I with a relatively sharp adsorption 'knee', which is typical for a mainly microporous material that has supermicropores and some small mesopores. When PPY is added to CNL carbon at a ratio of 1 : 2 (PPY : CNL carbon), the isotherm of the resulting sample (PPYCNL124) exhibits a much gentler 'knee' suggesting
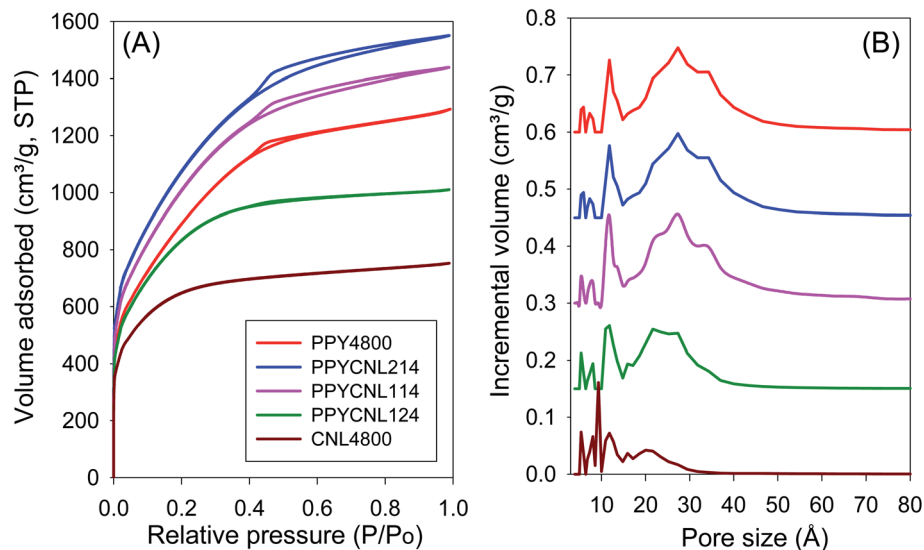
Fig. 1 (A) Nitrogen sorption isotherms and (B) pore size distribution curves of activated carbons derived from single precursor, PPY4800 (polypyrrole, PPY) and CNL4800 (CNL carbon) and from pre-mixed precursors containing PPY and CNL carbon at various weight ratios.

a greater proportion of mesopores. Further increase in the proportion of PPY in the pre-mixture results in activated carbons (PPYCNL114 and PPYCNL214) that exhibit type IV isotherms typical of mesoporous materials. Indeed, the isotherms of PPYCNL114 and PPYCNL214 are very similar to that of PPY4800, but with higher amounts of adsorbed nitrogen. The presence of CNL carbon in the pre-mixtures hinders the generation of mesoporosity to the extent that the isotherm of sample PPYCNL124 suggests a lack of any significant meso-porosity. The trends observed confirm that the nature of the pre-mix precursors has a major impact on the micropore/mesopore combination in the activated carbons. Indeed, semi-log plots of

the nitrogen sorption isotherms (Fig. S5A†) clearly evidence adsorption into the bi-modal pore systems of the pre-mixture derived carbons.

The nitrogen sorption isotherms and corresponding PSD curves for the PPY/ACDS set of samples, and the PPY-only derived sample (PPY4800) and ACDS-only derived sample (ACDS4800), are displayed in Fig. 2. The ACDS4800 sample has an isotherm that is typical of a microporous material. Use of a mix of PPY and ACDS as precursors generates activated carbons with isotherms whose shape and amount of nitrogen adsorbed is significantly altered compared to ACDS4800. Pre-mix precursors with a 1 : 2 (PPYDS124) or 1 : 1 (PPYDS114)
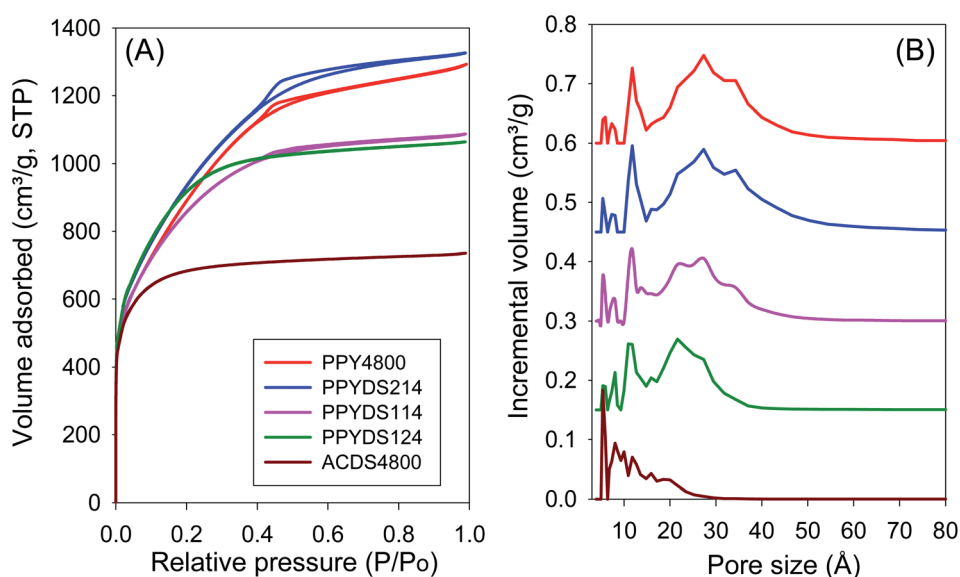

Fig. 2 (A) Nitrogen sorption isotherms and (B) pore size distribution curves of activated carbons derived from single precursor, PPY4800 (polypyrrole, PPY) and ACDS4800 (ACDS carbon) and from pre-mixed precursors containing PPY and ACDS carbon at various weight ratios.

ratio of PPY/ACDS generate activated carbons with isotherms that have a much gentler adsorption 'knee' consistent with the amount of PPY used. The isotherms of these two samples show a significant proportion of supermicropores and small mesopores that, in terms of the micropore/mesopore mix, lies between the levels of the PPY4800 and ACDS4800 samples. On the other hand, the isotherm of PPYDS214 is similar to that of PPY4800. It is clear to see that mixing polypyrrole and ACDS carbon in the precursor mix lowers mesoporosity, and that the amount of the reduction is greater for higher amounts of ACDS carbon.

The porosity data in Fig. 1 and 2 clearly shows that the nature of the precursors in the pre-mixtures determines the extent to which micropores or mesopores are generated in the activated carbons. Samples prepared from 1 : 2 mixture of PPY and CNL (PPYCNL124) or 1 : 2 and 1 : 1 mixtures of PPY and ACDS (PPYDS124 and PPYDS114) have a moderate level of mesoporosity, which, according to the isotherms, is somewhat intermediate between that of the biomass-derived (CNL4800 and ACDS4800) carbons and PPY4800. We interpret the lower mesoporosity in the pre-mix samples as arising from greater resistance to activation for the CNL and ACDS carbons. This is further clarified by considering the pore size maxima values (ESI Table S2†) determined from the pore size distribution curves in Fig. 1 and 2. The CNL-only sample (CNL4800) possess pores mainly within the micropore/supermicropore to small mesopore range, with most pores being of size below 20 Å and hardly any pores wider than 30 Å. The PPY-only (PPY4800) sample, on the other hand, exhibits bimodal pore size distribution with a small proportion of micropores centred at *ca.* 8 Å and 11 Å, and a much larger proportion of mesopores centred at *ca.* 34 Å. The pore size distribution of the PPY/CNL carbons differs significantly from that of PPY4800 and CNL4800. It is clear to see that the proportion and size of mesopores varies depending on the PPY : CNL ratio. The sample made from a 1 : 2 mixture of PPY/CNL carbon (PPYCNL124) has a relatively smaller proportion of mesopores centred at *ca.* 24 Å, which is

consistent with the observation that the sample tends towards being supermicroporous with small mesoporous and hardly any pores larger than 30 Å. On the other hand, the samples made from 1 : 1 or 2 : 1 mixture of PPY and CNL (PPYCNL114) and (PPYCNL214), contain a large proportion of mesopores centred at *ca.* 27 Å, and their pore size distribution is quite similar to that of PPY4800.

The ACDS-only (ACDS4800) sample possess a relatively wide size range of pores but still mainly within the micropore/supermicropore to small mesopore range, with most pores being of size below 20 Å and hardly any pores wider than 25 Å. The sample made from 1 : 2 or 1 : 1 mixture of PPY and ACDS (PPYDS124) or (PPYDS114) has a relatively smaller proportion of mesopores centred at 22 Å and 25 Å, respectively, which is consistent with the samples tending towards being supermicroporous with small mesoporous and hardly any pores larger than 30 Å. On the other hand, the samples made from a 2 : 1 mixture of PPY and ACDS (PPYDS214) contains a large proportion of mesopores centred at 27 Å, and has a pore size distribution similar to that of PPY4800. It can be concluded that the amount of PPY in the precursor mix is related to the presence of mesopores in the PPY/CNL or PPY/ACDS set of samples, and that the size of the mesopores varies based on the PPY : CNL or PPY : ACDS ratio. The quantity and size of mesopores vary, indicating that the pre-mixture has significant effect on the size of pores formed in activated carbons. Indeed, semi-log plots of the nitrogen sorption isotherms and PSD curves (Fig. S5A and B†) clearly evidence adsorption into the bi-modal pore systems of the carbons. The semi-log plots also show the balance between the contribution of micropores and mesopores to the porosity of the carbons, and the extent to which the nature and content of the pre-mix precursor determines the porosity.

The textural parameters of the activated carbons are summarised in Table 2. The PPY-only derived sample (PPY4800) has surface area of 3279 m² g⁻¹ and pore volume of 2.0 cm³ g⁻¹, while the CNL-only derived sample (CNL4800) has surface area

Table 2 Textural properties of activated carbons derived from single precursors (polypyrrole (PPY), CNL or ACDS carbon) and pre-mixtures of the precursors

Sample	Surface area $(m^2\ g^{-1})$	Micropore surface area[a] $(m^2\ g^{-1})$	Pore volume $(cm^3\ g^{-1})$	Micropore volume[b] $(cm^3\ g^{-1})$	Surface area density[c] $(m^2\ cm^{-3})$	Packing density[d] $(g\ cm^{-3})$	Volumetric surface area[e] $(m^2\ cm^{-3})$
PPY4800	3279	1320 (40%)	2.0	0.62 (31%)	1640	0.37	1213
CNL4800	2134	1819 (85%)	1.16	0.90 (78%)	1840	0.67	1430
PPYCNL124	2907	2215 (76%)	1.5	1.07 (71%)	1938	0.52	1512
PPYCNL114	3669	1741 (48%)	2.23	0.82 (37%)	1645	0.39	1431
PPYCNL214	3890	1717 (44%)	2.4	0.81 (34%)	1621	0.36	1400
ACDS4800	2609	1825 (70%)	1.1	0.70 (64%)	2372	0.69	1774
PPYDS124	3132	2631 (84%)	1.65	1.28 (78%)	1898	0.47	1472
PPYDS114	3101	2007 (65%)	1.7	0.93 (55%)	1824	0.47	1457
PPYDS214	3390	1372 (41%)	2.0	0.64 (32%)	1695	0.40	1356

[a] Values in parenthesis are % of surface area from micropores. [b] Values in parenthesis are % of pore volume from micropores. [c] Surface area density is obtained as ratio of total surface area to total pore volume. [d] The packing density was determined by pressing a given amount of carbon in a 1.3 cm die at pressure of 7 MPa for 5 min. Alternatively, relatively similar values are obtained using the general equation; $d_{carbon} = (1/\rho_s + V_T)^{-1}$ where ρ_s is skeletal density and V_T is total pore volume. [e] Volumetric surface area determined as surface area × packing density.

This journal is © The Royal Society of Chemistry 2022

J. Mater. Chem. A, 2022, **10**, 13744–13757 | **13749**

of 2134 m² g⁻¹ and pore volume of 1.16 cm³ g⁻¹. All the PPY/CNL carbons possess high or ultra-high surface areas which range between 2907 and 3890 m² g⁻¹, and pore volumes within the range of 1.5–2.40 cm³ g⁻¹. The highest surface area for a PPY/CNL sample is for PPYCNL214 (3890 m² g⁻¹) followed by PPYCNL114 (3669 m² g⁻¹), values that are higher than those for either the PPY-only (3279 m² g⁻¹) or CNL-only (2134 m² g⁻¹) derived carbons, and follow the trend in amount of PPY in the pre-mixture. The ACDS-only derived sample (ACDS4800) has a surface area of 2609 m² g⁻¹ and pore volume of 1.1 cm³ g⁻¹. The PPY/ACDS carbons possess moderate to high surface areas in the range 3101 to 3390 m² g⁻¹, and a pore volume of between 1.65 and 2.0 cm³ g⁻¹. The highest surface area is for PPYDS214 (3390 m² g⁻¹), which is greater than that for either PPY-only derived carbon (3279 m² g⁻¹) or ACDS-only derived carbon (2609 m² g⁻¹).

The addition of CNL and ACDS carbons to the mixtures increases microporosity and reduces the overall pore volume, with the reductions being greatest for samples prepared from 1 : 2 or 1 : 1 PPY/CNL or ACDS ratios (PPYCNL114, PPYDS124 and PPYDS114). The microporosity (given as % of surface area or pore volume from micropores) of activated carbons derived from pre-mix precursors decreases with the proportion of PPY in the mixtures. The textural data clearly demonstrate modulation of porosity of the activated carbons based only on systematic variation of the precursor mixtures. However, in all cases the proportion of microporosity does not go below that of the PPY4800 sample despite some of the samples having higher surface area and pore volume. It is also interesting to note that the data in Table 2 suggests that, in general, the textural parameters of the PPY/ACDS carbons are lower than for PPY/CNL equivalents, which is consistent with the fact that ACDS carbon has a lower O/C ratio (0.156) compared to CNL carbon (0.185).

Table 2 also gives the surface area density, which is defined as the ratio of total surface area to total pore volume, of the activated carbons. The surface area density is a parameter that can be used to assess any carbonaceous matter's susceptibility or resistance to activation as previously reported.[21,22] The surface area density of PPY4800, CNL4800 and ACDS4800 carbons is, respectively, 1640, 1840 and 2372 m² cm⁻³. The trend is consistent with the O/C ratio of the respective precursors, with low ratios signifying resistance to activation and therefore a higher surface area density.[21,22] ACDS4800 has the highest surface area density, which is consistent with the fact that the ACDS carbon is the most resistant to activation.[22] It has previously been shown that a high surface area density, i.e., the tendency to generate micropores as opposed to larger pores, arises because air-carbonisation of biomass enriches the proportion of lignin products, which are less susceptible to activation.[18–21,39–45] This confirms that the O/C ratio is an inherent property of the starting carbonaceous material and that it can be used as a predictor of activation resistance and therefore, ultimately, the type of porosity to be generated.

The surface area density of the pre-mix activated carbons is in the range 1621–1938 m² cm⁻³. Activated carbons derived from pre-mixtures with high amounts of PPY have a lower surface area density, i.e., the surface area density is inversely proportional to the amount of PPY in the pre-mixture. In particular, samples PPYCNL114, PPYCNL214 and PPYDS214, which are lowly microporous (i.e., have the highest proportion of mesoporosity), display lower surface area density of 1621, 1645 and 1695 m² cm⁻³, respectively. However, the surface area density of these samples is still higher or comparable to that of PPY4800. Indeed, only sample PPYCNL214, with an extremely high surface area of close to 3900 m² g⁻¹, has surface area density lower than that of PPY4800. Due to their microporous nature, sample CNL4800 and ACDS4800 have relatively high packing density of 0.67 and 0.69 g cm⁻³, respectively, which is significantly higher than that (0.37 g cm⁻³) of the more mesoporous PPY4800. The packing density of the pre-mix activated carbons is between 0.36 and 0.52 g cm⁻³. It is noteworthy that despite the higher porosity of some of the pre-mix samples (PPYCNL114, PPYCNL214 and PPYDS214), their packing density is higher or similar to that of PPY4800. This is attributed to the packing density enhancing contribution of the CNL and ACDS carbon ingredients.

The volumetric surface area (defined as surface area × packing density) of the carbons in Table 2 shows some interesting trends. We note that volumetric surface area of porous materials has previously been used as a measure of gas storage performance especially for methane.[22,46] The volumetric surface area of PPY4800, CNL4800 and ACDS4800 carbons is, respectively, 1213, 1430 and 1774 m² cm⁻³. Once again, the trend is consistent with the O/C ratio of the respective precursors, with low ratios resulting in activated carbons with higher volumetric surface area. The volumetric surface area of the pre-mix activated carbons is in the range 1400–1512 m² cm⁻³ for PPYCNL carbons and between 1356 and 1472 m² cm⁻³ for PPYDS samples. The volumetric surface area is inversely proportion to the amount of PPY in the pre-mixture, and consequently reduces for samples that have a high proportion of mesoporosity. It is noteworthy that the volumetric surface area of all pre-mix samples, including those with very high surface area (PPYCNL114, PPYCNL214 and PPYDS214) is higher than that of PPY4800. Moreover, the volumetric surface area of the present pre-mix carbons is amongst the highest reported for porous materials.[22,47,48] MOFs have been reported to have higher volumetric surface area (e.g., 2060 m² cm⁻³ for NU-1501-Al) but such values are likely to be an overestimation as they are computed using crystallographic density rather than packing density.[47]

To get further insights on the trends discussed above, it is useful to consider the behaviour of a variety of carbonaceous matter with variable O/C ratio in order to more fully understand the effect of elemental composition, particularly the O/C ratio, on the activation of various precursors and the generation of mesoporosity. In this regard, the porosity of PPY4800, CNL4800 and ACDS4800 was compared to that of previously reported activated carbons derived from raw sawdust, sawdust-derived hydrochar[21] and Jujun grass.[25] All carbonaceous precursors were activated in a similar manner, i.e., at 800 °C and KOH/precursor ratio of 4. The O/C ratio of the precursors varied between 0.156 and 0.773 in the order: raw sawdust > Jujun grass > sawdust hydrochar > CNL carbon > flash air-carbonised date

13750 | J. Mater. Chem. A, 2022, 10, 13744–13757

This journal is © The Royal Society of Chemistry 2022

seed (ACDS). The porosity data (ESI Table S3†) demonstrates a link between the O/C ratio of the precursors and the degree of mesoporosity generated in the activated carbons. The carbonaceous precursors with high O/C ratio generated activated carbons, *e.g.* SD4800D and ACGR-4800, with greater mesoporosity. In contrast, the porosity of activated carbons obtained from precursors with a low O/C ratio, *e.g.* CNL4800 and ACDS4800, exhibited low levels of mesoporosity. The level of mesoporosity is, therefore, a measure of the ease with which the precursors can be activated; high O/C ratio precursors can be activated more rapidly or to a greater degree to generate larger pores, whereas low O/C precursors are more resistant to KOH activation and hence predominantly yield micropores. Thus, samples ACDS4800 and CNL4800 are almost totally microporous with microporosity of 70% and 85%, respectively, whereas sample PPY4800 has only 40% microporosity. Furthermore, a previous study reported an inability to directly activate cellulose acetate, which has a high O/C ratio of 0.93, and had no carbon yield on activation.[23,28] The absence of any yield signifies complete burn-off since cellulose acetate is most readily activated as a consequence of its high O/C ratio. Regarding the effect of a high O/C ratio on the activation process, it is likely that a higher O content means a higher proportion of O-containing polar functional groups, which makes activation easier. A low O/C ratio, on the other hand, is related to the presence of stable carbon forms that are resistant to activation.[26]

3.3 Methane storage

In order for a porous material to achieve efficient methane storage at moderate to high pressures, *e.g.* 35–100 bar, it should be essentially microporous with low mesoporosity and a large surface area. Pore channel dimensions with a diameter of 8 to 15 Å offer the most efficient adsorption of 2 or 3 methane molecules whilst optimising the packing of the adsorbed phase within the pores.[4–9,46,47] The present carbons should be ideal candidates to attain high methane storage capacity at moderate to high pressures, particularly given their combination of micro- and mesoporous characteristics. The methane uptake capacity of the carbons was determined at pressures of between 0 and 100 bar, and at ambient temperature, *i.e.*, 25 °C. Focus was placed on uptake at 35, 65 and 100 bar, pressures that have been widely benchmarked in previous studies and which allow for easy comparison of the performance of the present carbons to current state-of-the-art materials. The methane uptake measurements facilitated direct determination of the excess uptake. The total methane storage capacity was then determined from the excess data by considering the density of methane at any temperature and pressure and the total pore volume of the adsorbing activated carbon. This was achieved by applying the equation:

$$\theta_T = \theta_{Exc} + d_{CH4} \times V_T$$

where; θ_T is total methane uptake, θ_{Exc} is excess methane uptake, d_{CH4} is density (g cm^{-3}) of methane gas under the prevailing temperature and pressure, and V_T is total pore volume (cm^3 g^{-1}) of the activated carbon. The methane density (d_{CH4}) was obtained from the National Institute of Standards and Technology website (https://www.nist.gov/).

Fig. 3 shows the excess methane uptake isotherms of PPY4800, CNL4800 and ACDS4800 along with those of the PPY/CNL and PPY/ACDS pre-mix carbons. Table 3 summarises the methane storage capacity at 35, 65 and 100 bar. For all the activated samples, the methane uptake isotherms are completely reversible with no hysteresis. At 35 bar, PPY4800 stores 12.6 mmol g^{-1} whereas CNL4800 and ACDS4800 store 11.1 and 10.9 mmol g^{-1}, respectively. For the PPY/CNL samples, the methane storage capacity at 35 bar is between 11.8 and 12.7 mmol g^{-1}, while for the PPY/ACDS carbons it varies 11.8
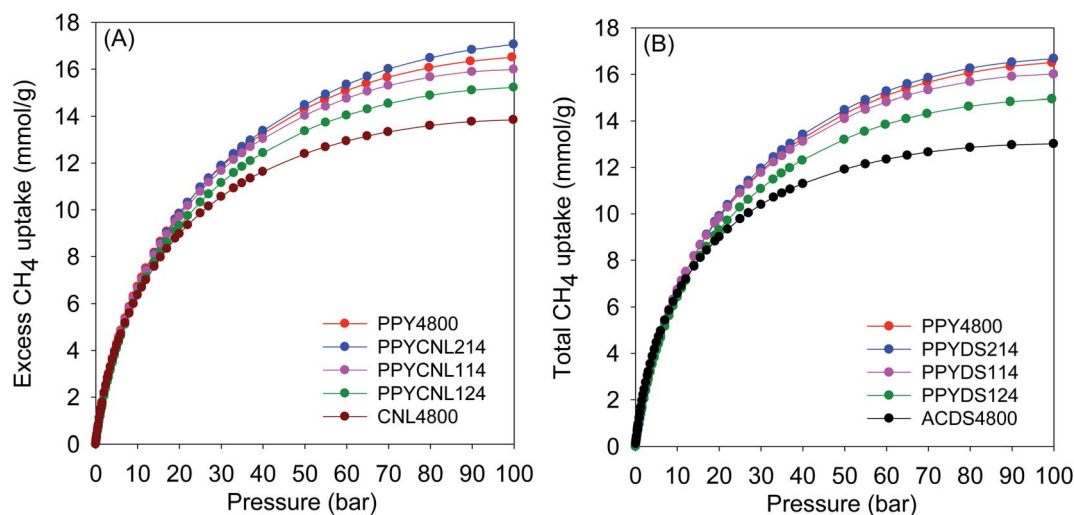

Fig. 3 Excess gravimetric methane uptake of activated carbons derived from single precursor, PPY4800 (polypyrrole, PPY), CNL4800 (CNL carbon) and ACDS4800 (ACDS carbon) and from pre-mixed precursors containing PPY and (A) CNL carbon or (B) ACDS carbon at various weight ratios.

Journal of Materials Chemistry A

Table 3 Excess gravimetric methane uptake of activated carbons derived from single precursor, PPY4800 (polypyrrole, PPY) and CNL4800 (CNL carbon) and from pre-mixed precursors containing PPY and CNL carbon at various weight ratios

Sample	Excess gravimetric methane uptake (mmol g^{-1})		
	35 bar	65 bar	100 bar
PPY4800	12.6	15.4	16.5
CNL4800	11.1	13.2	13.9
PPYCNL124	11.8	14.3	15.2
PPYCNL114	12.4	15.1	16.0
PPYCNL214	12.7	15.7	17.1
ACDS4800	10.9	12.5	13.0
PPYDS124	11.8	14.1	15.0
PPYDS114	12.5	15.1	16.0
PPYDS214	12.8	15.6	16.7

and 12.8 mmol g^{-1}. The excess methane uptake is generally in line with the surface area of the carbons. At 25 °C and 35 bar, excess methane uptake of up to 12.8 mmol g^{-1} is amongst the highest reported for any porous material and shows the potential of the pre-mix carbons as methane stores at moderate pressure.[4–9,46,47,49–51] The excess methane uptake of the pre-mixed carbons is in the range of 14.1–15.7 mmol g^{-1} and 15.0–17.1 mmol g^{-1} at 65 and 100 bar, respectively, with samples PPYCNL214 and PPYDS214 having the highest methane uptake. It is clear that samples prepared from pre-mixtures with a higher amount of PPY store greater amounts of methane, which surpasses that of single precursor carbons (PPY4800, CNL4800 and ACDS4800). This is the first indication that the strategy of using pre-mixtures as precursors, which transfers to modulated porosity, also has a positive effect on methane storage capacity.

From the data in Fig. 3 and Table 3, the excess gravimetric methane uptake appears to be determined by several factors: (i) the level of microporosity, which appears to have an inverse relationship with the excess methane uptake; (ii) the total surface area, with excess methane uptake increasing for higher surface area carbons; and (iii) the nature of the pre-mixture with greater amounts of PPY being associated with increased methane uptake due to higher surface area. To get a clearer view of the methane storage efficiency, we explored the methane uptake density (expressed as mmol CH$_4$ m^{-2}) of the carbons (ESI Fig. S6†). For PPY/CNL carbons, the uptake density appears to be related to the level of microporosity with sample CNL4800 having both the highest density and micropore surface area, followed by PPYCNL124. There is little variation in the uptake density of PPY4800 and the PPY/CNL samples, which is line with the pore maxima of these carbons (Table S2†) with pores of size 12 Å and 23–27 Å. The higher uptake density of CNL4800 may be related to the presence of significant proportion of pores of size 8–10 Å, which is consistent with previous reports that 8 to 11 Å diameter pores are within the pore range that offer the most efficient adsorption of methane with optimised packing of the adsorbed phase within the pores.[4–9,46,47,52] For PPYDS samples (Fig. S6B†), there is only a slight link to the level of microporosity. It is surprising that the uptake density of ACDS4800 is only slightly higher (especially at low pressure (Fig. S7†) than that of the PPY/DS samples. This may be explained by the fact that ACDS4800 is unique in having a significant proportion of 6 Å pores and that such pores are not efficient for high density methane storage as they are too small to optimise packing of 2 or 3 CH$_4$ molecules. This is consistent with previous reports that pores of size 11 Å are the most suited for methane storage.[52]

The total gravimetric methane uptake isotherms of PPY4800, CNL4800 and ACDS4800 along with those of the PPY/CNL and PPY/ACDS carbons are shown in Fig. 4. The total gravimetric
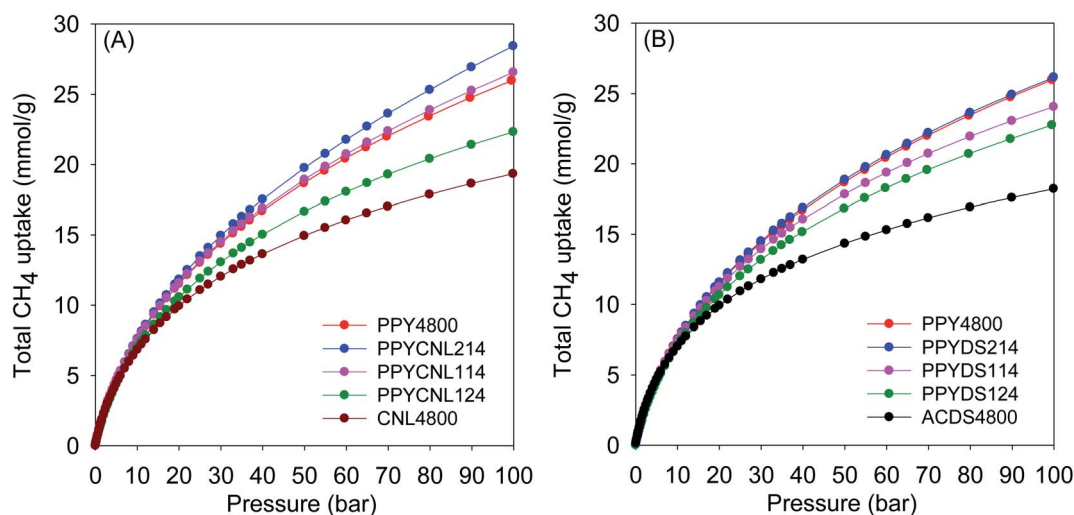

Fig. 4 Total gravimetric methane uptake of activated carbons derived from single precursor, PPY4800 (polypyrrole, PPY), CNL4800 (CNL carbon) and ACDS4800 (ACDS carbon) and from pre-mixed precursors containing PPY and (A) CNL carbon or (B) ACDS carbon at various weight ratios.

Table 4 Total gravimetric methane uptake of activated carbons derived from single precursor, PPY4800 (polypyrrole, PPY) and CNL4800 (CNL carbon) and from pre-mixed precursors containing PPY and CNL carbon at various weight ratios

Sample	Total gravimetric methane uptake (mmol g^{-1})		
	35 bar	65 bar	100 bar
PPY4800	15.6	21.2	26.0
CNL4800	12.9	16.6	19.3
PPYCNL124	14.1	18.7	22.3
PPYCNL114	15.8	21.6	26.6
PPYCNL214	16.3	22.7	28.4
ACDS4800	12.6	15.7	18.2
PPYDS124	14.2	18.9	22.8
PPYDS114	15.1	20.1	24.1
PPYDS214	15.8	21.4	26.1

methane uptake at 35, 65 and 100 bar, is summarised in Table 4 and generally follow the trends discussed above for the excess uptake. For the single precursor materials, the total methane storage was, respectively for PPY4800, CNL4800 and ACDS4800, 15.6, 12.9 and 12.6 mmol g^{-1} (at 35 bar) 21.2, 16.6 and 15.7 mmol g^{-1} (at 65 bar) and 26.0, 19.3 and 18.2 mmol g^{-1} (at 100 bar). For PPY/CNL carbons the total methane uptake at 35 bar varies from 14.1 to 16.3 mmol g^{-1}, while for PPY/DS samples it is between 14.2 and 15.8 mmol g^{-1}. The mixed precursors offer carbons with total gravimetric methane uptake that outperforms previously reported carbon materials.[10,53–55] Moreover, the total gravimetric uptake of some of the pre-mixed carbons also surpasses that of PPY4800. At 65 bar, the total methane uptake varies from 18.7 to 22.7 mmol g^{-1} for PPY/CNL carbons, and is between 18.9 and 21.4 mmol g^{-1} for PPY/DS samples. At 100 bar, the total methane uptake varies from 22.2 to 28.4 mmol g^{-1} for PPY/CNL carbons, and ranges from 22.8 to 26.1 mmol g^{-1} for PPY/DS samples. Such gravimetric

uptake is amongst the best reported to date for carbon or MOF materials.[4–10,49–58]

A gravimetric methane uptake target of 0.5 g g^{-1} has been set by the US DOE. The uptake of some of the pre-mix samples (ESI Table S4†) is very close to the DOE target; 0.43 g g^{-1} (PPYCNL114), 0.46 g g^{-1} (PPYCNL214) and 0.42 g g^{-1} (PPYDS214). These values, along with that of PPY4800 (0.42 g g^{-1}) are higher that any previously reported for carbons and are comparable to the best of other materials such as MOFs.[4–10,49–58] It is noteworthy that while the pre-mix samples have uptake that is comparable or better than that of PPY4800, they have much higher gravimetric storage than CNL4800 and ACDS4800 by up to 25% (35 bar), 40% (at 65 bar) and 50% (at 100 bar). Such gravimetric uptake, if coupled with good volumetric uptake, would make the pre-mix samples very attractive for methane storage.

At 25 °C and up to 100 bar, the targeted porosity development in the pre-mix carbons clearly achieves excellent gravimetric methane storage capacity. The volumetric uptake, which takes into account an adsorbent's packing density, is a key measure of methane storage performance and is defined as cm^3 (STP) cm^{-3}, i.e., cm^3 of methane per unit tank volume occupied by the adsorbent. Along with the gravimetric uptake target mentioned above (0.5 g g^{-1}), the US DOE has set a target of 263 cm^3 (STP) cm^{-3} at 25 °C and moderate pressure, i.e., 35–100 bar. Fig. 5 shows the total volumetric methane storage isotherms, and Table 5 summarises the uptake at 35, 65 and 100 bar. Table 5 also gives the working capacity (i.e., deliverable methane) defined as the difference in uptake between 5 bar and the storage pressure (35, 65 or 100 bar). For the single precursor materials, the total methane volumetric storage (cm^3 (STP) cm^{-3}) was, respectively, for PPY4800, CNL4800 and ACDS4800, 129, 194 and 194 (at 35 bar) 176, 249 and 243 (at 65 bar) and 215, 291 and 282 (at 100 bar). The total volumetric capacity for PPY/CNL carbons at 35 bar varies from 132 to 164 at 35 bar, while for PPY/DS samples it is in the range 141 to 159. It is noteworthy that
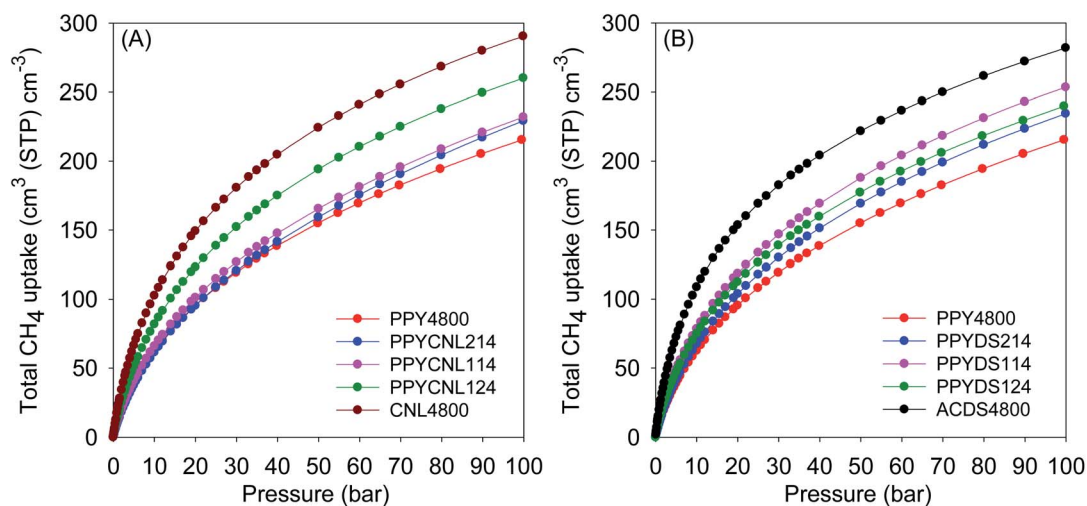

Fig. 5 Total volumetric methane uptake of activated carbons derived from single precursor, PPY4800 (polypyrrole, PPY), CNL4800 (CNL carbon) and ACDS4800 (ACDS carbon) and from pre-mixed precursors containing PPY and (A) CNL carbon or (B) ACDS carbon at various weight ratios.

This journal is © The Royal Society of Chemistry 2022

J. Mater. Chem. A, 2022, **10**, 13744–13757 | **13753**

Table 5 Total volumetric methane uptake and working capacity of activated carbons derived from single precursor, PPY4800 (polypyrrole, PPY) and CNL4800 (CNL carbon) and from pre-mixed precursors containing PPY and CNL carbon at various weight ratios

Sample	Total volumetric methane uptake[a] (cm^3 (STP) cm^{-3})		
	35 bar	65 bar	100 bar
PPY4800	129 (90)	176 (137)	215 (177)
CNL4800	194 (127)	249 (182)	291 (224)
PPYCNL124	164 (113)	217 (167)	260 (209)
PPYCNL114	138 (97)	189 (148)	232 (191)
PPYCNL214	132 (94)	183 (146)	229 (192)
ACDS4800	194 (122)	243 (171)	282 (209)
PPYDS124	150 (103)	199 (152)	240 (193)
PPYDS114	159 (110)	211 (162)	254 (205)
PPYDS214	141 (100)	192 (151)	234 (193)

[a] The values in parenthesis are the volumetric working capacity defined as the difference in uptake between the stated pressure (35, 65 or 100 bar) and 5 bar.

that, in all cases, the total volumetric uptake of the pre-mixed carbons surpasses that of PPY4800. At 65 bar, the total methane uptake varies from 183 to 217 cm^3 (STP) cm^{-3} for PPY/CNL carbons, and 199–211 cm^3 (STP) cm^{-3} for PPY/DS samples. At 100 bar, the total methane uptake varies from 229 to 260 cm^3 (STP) cm^{-3} for PPY/CNL carbons, and from 234 to 254 cm^3 (STP) cm^{-3} for PPY/DS samples. Such volumetric uptake, calculated based on experimentally determined packing density, is amongst the best reported to date for carbon or MOF materials.[4–10,49–58]

In all cases, the volumetric uptake of the pre-mix samples outperform that of PPY4800. This is due to the low packing density of PPY4800 arising from a highly mesoporous nature. Thus despite a high gravimetric uptake, the performance of PPY4800 is limited by low volumetric uptake and working capacity. On the other hand, some of the pre-mix samples have

impressive volumetric uptake in addition to high gravimetric storage capacity. Although samples CNL4800 and ACDS4800 have the highest volumetric uptake, their performance is compromised by low gravimetric uptake that only reaches ca. 0.3 g g^{-1} at 100 bar. It is interesting to note that the volumetric uptake of the best performing pre-mix samples is only 10–20% lower than that of CNL4800 and ACDS4800 but with comparable volumetric working capacity despite gravimetric uptake that is up to 50% higher. The pre-mix samples, therefore, offer optimised performance as methane stores with respect to the balance between gravimetric and volumetric storage capacity.

A positive consequence, on methane uptake of lowering the mesoporosity in comparison to PPY4800 has been achieved. Whilst the highest total volumetric methane uptake was exhibited by samples with the greatest microporosity and the highest packing density, i.e., CNL4800 and ACDS4800, these samples have low gravimetric uptake. The decreased mesoporosity of the pre-mix precursor samples, compared to PPY4800, offers the benefit of increased packing density. As discussed above, packing density is inversely related to pore volume. The packing density of porous solids is critical for their use as methane stores since it dictates how much gas can be kept in a limited space, such as a storage tank, when the material is packed to its full volumetric storage capacity. Storage materials therefore need to fulfil both gravimetric and volumetric storage targets, which is demonstrated by the best performing pre-mix samples. For example, the best performing porous carbons reported to date for total volumetric methane storage at 25 °C and 35 bar are mesophase pitch derived activated carbons, LMA738 (165 cm^3 cm^{-3}) and DO00-3:1_700 (184 cm^3 cm^{-3}), zeolite templated carbons, ZTC, (BEA-ZTC) that stores 148 cm^3 cm^{-3} and thermally treated BEA-ZTC (BEA-ZTC-873) that stores 165 cm^3 cm^{-3} (ESI Table S5†). In comparison, the present pre-mixed carbons have comparable volumetric uptake but much higher gravimetric storage capacity.

The isosteric heat of adsorption (Q_{st}) for the carbons (ESI Fig. S8†) was found to be in the range of 19–14 kJ mol^{-1} at
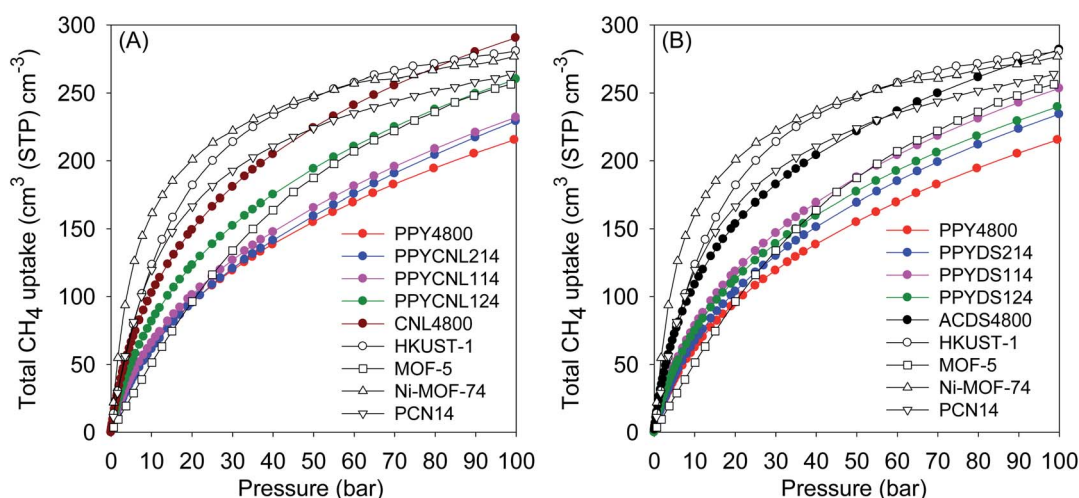

Fig. 6 Total volumetric methane uptake of activated carbons derived from single precursors (PPY4800, CNL4800, ACDS4800) or (A) PPY/CNL or (B) PPY/DS pre-mixtures compared to benchmark MOF materials. The uptake of MOFs was calculated using crystallographic density.

13754 | J. Mater. Chem. A, 2022, 10, 13744–13757

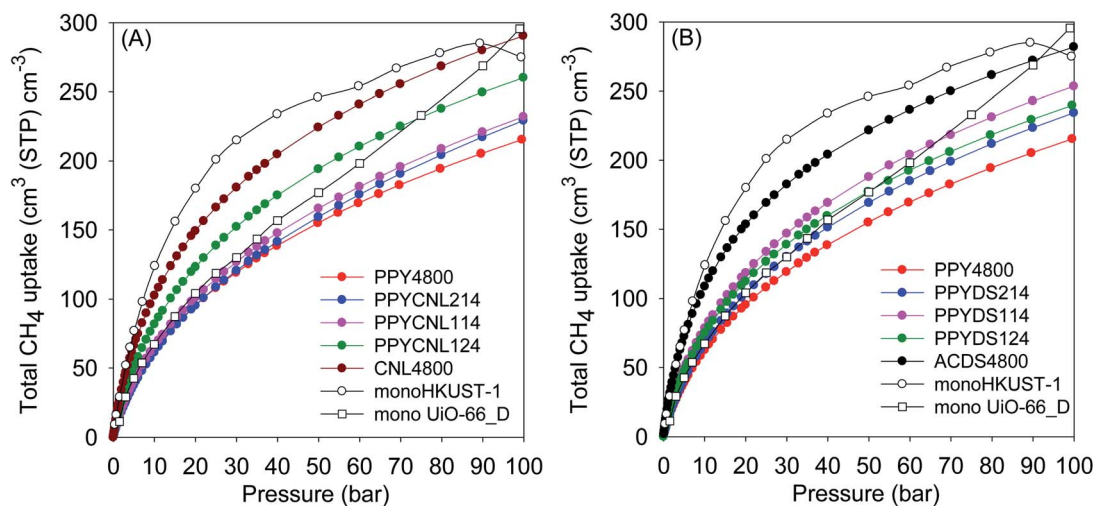This journal is © The Royal Society of Chemistry 2022

Fig. 7 Total volumetric methane uptake of activated carbons derived from single precursors (PPY4800, CNL4800, ACDS4800) or (A) PPY/CNL pre-mixtures or (B) PPY/DS pre-mixtures compared to storage capacity of monolithic $_{mono}$HKUST-1 and $_{mono}$UiO-66_D.

methane loading of up to 6 mmol g^{-1}. This range is in line with Q_{st} observed for activated carbons, which has been previously reported to typically range from 10 to 25 kJ mol^{-1} depending on methane loading.[59] The Q_{st} reduces significantly at low uptake and then the decrease stabilises at higher loading (>1 mmol g^{-1}). We observed no link between the Q_{st} and methane uptake, which confirms that the uptake is mainly determined by the porosity of the carbons. Our discussion, therefore, focusses further on the trends between porosity and methane uptake.

For a more comprehensive understanding of the methane storage performance of the present carbons, their performance was compared to current benchmark materials. Metal organic frameworks (MOFs) have been reported as the current record holders for methane storage in powdered solids. Fig. 6 shows a comparison between the present carbons and benchmark MOFs, namely, HKUST-1, Ni-MOF-74, Co-MOF-74 and PCN-14.[4–9,60] The volumetric uptake of the present carbons is comparable to the benchmark materials even when crystal density is used to calculate the uptake of the MOFs. The use of crystallographic density leads to overestimated volumetric uptake values and suggest impractical scenarios requiring that MOFs be packed as single crystals into confined spaces such as storage tanks/cylinders. The reality is that MOF packing density is often substantially lower (up to 50% lower) than its crystallographic density.[46] As a result, when used in real-world applications, volumetric uptake of MOFs is expected to reduce by 25 to 50%, meaning that they would actually be mostly lower than for the present carbons (ESI Fig. S9†). The performance of the present carbons is, in particularly, significantly higher at pressures above 50 bar (Fig. S9†).

A more realistic comparison that avoids the ambiguity associated with the use of crystallographic density (for MOFs) is the recent work of Tian and co-workers who reported on monolithic MOFs, designated as $_{mono}$HKUST-1, which have high packing density (1.06 g cm^{-3}) and enhanced volumetric methane uptake.[46] The $_{mono}$HKUST-1 and related monolithic MOFs, such as the more practical $_{mono}$UiO-66_D, are the current record holders for methane storage at 25 °C and pressure of up to 100 bar.[46,56] In Fig. 7, performance of the present carbons is compared to that of $_{mono}$HKUST-1 and $_{mono}$UiO-66_D. The volumetric uptake of the present carbons is impressive over the full pressure range and is better or comparable to that of $_{mono}$UiO-66_D. The uptake of the carbons is lower than that of $_{mono}$HKUST-1, which is better than any other MOF reported to date.[46] The comparison in Fig. 7 illustrates the attraction of the present carbons as practical methane stores given that they can be readily prepared *via* low cost routes. A further attraction of the present carbons is that they have much higher gravimetric uptake compared to $_{mono}$HKUST-1 and $_{mono}$UiO-66_D (ESI Fig. S10†).

For a desorption pressure of 5 bar, the present carbons show good working capacity that is comparable to that of $_{mono}$HKUST-1 and $_{mono}$UiO-66_D (Table S6†). Although $_{mono}$HKUST-1 is the current record holder for volumetric methane storage in porous materials and is claimed to be 50% better than any other MOF, its practical use is limited by relatively low working capacity and the need to mitigate chemical instability associated with loss of crystallinity when exposed to moisture.[46,56] The more relevant comparison for the present carbons is, therefore, with the more robust and stable $_{mono}$UiO-66_D. At 35 bar, the total volumetric uptake and working capacity of the carbons is better than that of $_{mono}$UiO-66_D (Table S6†). At 65 bar, the performance of the carbons is comparable to that of $_{mono}$UiO-66_D. Only at the much higher pressure of 100 bar is the working capacity of $_{mono}$UiO-66_D slightly higher than that of the best carbons.

4. Conclusions

Pre mixtures of polypyrrole (PPY) with biomass derived CNL carbon or ACDS carbon, were successfully used to modulate the porosity of activated carbons. The use of pre-mixed precursors enabled the relationship between level of activation and surface

This journal is © The Royal Society of Chemistry 2022

J. Mater. Chem. A, 2022, **10**, 13744–13757 | **13755**

area to be optimised in a manner that cannot be achieved with single precursors. Thus, the pre-mixed precursors provide carbon materials with ultra-high surface area and pore volume, *i.e.* of up to 3890 m^2 g^{-1} and 2.40 cm^3 g^{-1}, respectively. The porosity of pre-mixed carbons is primarily made up of micropores (6–12 Å) and small mesopores (20–30 Å). The combination of mesoporosity, arising from PPY, and microporosity from the biomass sources (CNL or ACDS carbons) means that the porosity of the pre-mix carbons can be readily tailored to exhibit varying combinations of micropores, supermicropores and small mesopores. This is achieved under identical activation conditions, *i.e.* 800 °C and a KOH/precursor ratio of 4, wherein the porosity is only modulated by the amount of PPY and the biomass – derived carbons in the precursor. This study offers further evidence that the elemental composition of the precursors (*i.e.*, carbonaceous starting materials), and in particular the molar ratio of oxygen to carbon (*i.e.*, O/C molar ratio), is the genesis of the ability to modulate porosity. A high O/C ratio favours ease of activation and the formation of mesopores, while a low ratio is associated with resistance to activation and the formation of micropores. We show that knowledge of the O/C ratio of carbonaceous matter allows prediction of activation behaviour, porosity, and micropore/mesopore mix. The carbons developed in this study are excellent stores for methane owing to their tailored porosity and packing density. The methane storage performance of the carbons is better than all previously reported carbons and powder MOFs, and only comparable to that of monolithic MOFs that are the current record holders for volumetric methane storage in porous solids.

Conflicts of interest

There are no conflicts to declare.

Acknowledgements

References

1 U. Eberle, B. Muller and R. von Helmot, *Energy Environ. Sci.*, 2012, **5**, 8780.

2 M. E. Boot-Handford, J. C. Abanades, E. J. Anthony, M. J. Blunt, S. Brandani, N. Mac Dowell, J. R. Fernandez, M. C. Ferrari, R. Gross, J. P. Hallett, R. S. Haszeldine, P. Heptonstall, A. Lyngfelt, Z. Makuch, E. Mangano, R. T. J. Porter, M. Pourkashanian, G. T. Rochelle, N. Shah, J. G. Yao and P. S. Fennell, *Energy Environ. Sci.*, 2014, **7**, 130.

3 K. Z. House, A. C. Baclig, M. Ranjan, E. A. van Nierop, J. Wilcox and H. J. Herzog, *Proc. Natl. Acad. Sci. U. S. A.*, 2011, **108**, 20428.

4 T. A. Makal, J. R. Li, W. Lu and H. C. Zhou, *Chem. Soc. Rev.*, 2012, **41**, 7761.

5 J. A. Mason, M. Veenstra and J. R. Long, *Chem. Sci.*, 2014, **5**, 32.

6 K. V. Kumar, K. Preuss, M. M. Titirici and F. Rodriguez-Reinoso, *Chem. Rev.*, 2017, **117**, 1796.

7 B. Li, H.-M. Wen, W. Zhou, J. Q. Xu and B. Chen, *Chem*, 2016, **1**, 557.

8 S. Dutta, A. Bhaumik and K. C.-W. Wu, *Energy Environ. Sci.*, 2014, **7**, 3574.

9 Y. He, W. Zhou, G. Qian and B. Chen, *Chem. Soc. Rev.*, 2014, **43**, 5657.

10 M. E. Casco, M. Martínez-Escandell, E. Gadea-Ramos, K. Kaneko, J. Silvestre-Albero and F. Rodríguez-Reinoso, *Chem. Mater.*, 2015, **27**, 959.

11 I. Angelidaki, L. Treu, P. Tsapekos, G. Luo, S. Campanaro, H. Wenzel and P. Kougias, *Biotechnol. Adv.*, 2018, **36**, 452.

12 Z. Bacsik, O. Cheung, P. Vasiliev and N. Hedin, *Appl. Energy*, 2016, **162**, 613.

13 M. I. Khan, T. Yasmin and A. Shakoor, *Renewable Sustainable Energy Rev.*, 2015, **51**, 785.

14 M. Namvar-Asl, M. Soltanieh and A. Rashidi, *Energy Convers. Manage.*, 2008, **49**, 2478.

15 M. Feroldi, A. C. Neves, C. E. Borba and H. J. Alves, *J. Cleaner Prod.*, 2018, **172**, 921.

16 M. Sevilla and R. Mokaya, *Energy Environ. Sci.*, 2014, **7**, 1250.

17 Z. Hu, M. P. Srinivasan and Y. Ni, *Carbon*, 2001, **39**, 877.

18 E. Haffner-Staton, N. Balahmar and R. Mokaya, *J. Mater. Chem. A*, 2016, **4**, 13324.

19 N. Balahmar, A. S. Al-Jumialy and R. Mokaya, *J. Mater. Chem. A*, 2017, **5**, 12330.

20 E. A. Hirst, A. Taylor and R. Mokaya, *J. Mater. Chem. A*, 2018, **6**, 12393.

21 N. Balahmar and R. Mokaya, *J. Mater. Chem. A*, 2019, **7**, 17466.

22 A. Altwala and R. Mokaya, *Energy Environ. Sci.*, 2020, **13**, 2967.

23 T. S. Blankenship, N. Balahmar and R. Mokaya, *Nat. Commun.*, 2017, **8**, 1545.

24 W. Sangchoom and R. Mokaya, *ACS Sustainable Chem. Eng.*, 2015, **3**, 1658.

25 H. M. Coromina, D. A. Walsh and R. Mokaya, *J. Mater. Chem.*, 2016, **4**, 280.

26 X. Zhu, Y. Liu, F. Qian, C. Zhou, S. Zhang and J. Chen, *ACS Sustainable Chem. Eng.*, 2015, **3**, 833.

27 M. Sevilla, W. Sangchoom, N. Balahmar, A. B. Fuertes and R. Mokaya, *ACS Sustainable Chem. Eng.*, 2016, **4**, 4710.

28 T. S. Blankenship and R. Mokaya, *Energy Environ. Sci.*, 2017, **10**, 2552.

29 M. Sevilla, R. Mokaya and A. B. Fuertes, *Energy Environ. Sci.*, 2011, **4**, 2930.

30 M. Sevilla, P. Valle-Vigon and A. B. Fuertes, *Adv. Funct. Mater.*, 2011, **21**, 2781.

13756 | *J. Mater. Chem. A*, 2022, **10**, 13744–13757

This journal is © The Royal Society of Chemistry 2022

31 N. Balahmar, A. C. Mitchell and R. Mokaya, *Adv. Energy Mater.*, 2015, **5**, 1500867.

32 B. Adeniran and R. Mokaya, *Nano Energy*, 2015, **16**, 173.

33 M. Cox and R. Mokaya, *Sustainable Energy Fuels*, 2017, **1**, 1414.

34 J. S. M. Lee, M. E. Briggs, T. Hasell and A. I. Cooper, *Adv. Mater.*, 2016, **28**, 9804.

35 F. Rouquerol, J. Rouquerol and K. Sing, *Adsorption by Powders and Porous Solids: Principles, Methodology and Applications*, Academic Press, San Diego, 1999.

36 P. C. Hansen and D. P. O'Leary, *SIAM J. Sci. Comput.*, 1993, **14**, 1487.

37 P. C. Hansen, *SIAM Rev.*, 1992, **34**, 561.

38 I. M. Minisy, U. Acharya, L. Kobera, M. Trchová, C. Unterweger, S. Breitenbach, J. Brus, J. Pfleger, J. Stejskal and P. Bober, *J. Mater. Chem. C*, 2020, **8**, 12140.

39 M. J. Antal, E. Croiset, X. Dai, C. DeAlmeida, W. S.-L. Mok, N. Norberg, J.-R. Richard and M. Al Majthoub, *Energy Fuels*, 1996, **10**, 652.

40 M. J. Antal, S. G. Allen, X. Dai, B. Shimizu, M. S. Tam and M. Gronli, *Ind. Eng. Chem. Res.*, 2000, **39**, 4024.

41 W. M. A. W. Daud and W. S. W. Ali, *Bioresour. Technol.*, 2004, **93**, 63.

42 H. Yang, R. Yan, H. Chen, C. Zheng, D. H. Lee and D. T. Liang, *Energy Fuels*, 2006, **20**, 388.

43 M. Bbebu and C. Vasile, *Cellul. Chem. Technol.*, 2010, **44**, 353.

44 R. K. Sharma, J. B. Wooten, V. L. Baliga, X. Lin, W. G. Chan and M. R. Hajaligol, *Fuel*, 2004, **83**, 1469.

45 Z. Fang, T. Sato, R. L. Smith Jr, H. Inomata, K. Arai and J. A. Kozinski, *Bioresour. Technol.*, 2008, **99**, 3424.

46 T. Tian, Z. Zeng, D. Vulpe, M. E. Casco, G. Divitini, P. A. Midgley, J. Silvestre-Albero, J.-C. Tan, P. Z. Moghadam and D. Fairen-Jimenez, *Nat. Mater.*, 2018, **17**, 174.

47 Z. Chen, P. Li, R. Anderson, X. Wang, X. Zhang, L. Robison, L. R. Redfern, S. Moribe, T. Islamoglu, D. A. Gómez-Gualdrón, T. Yildirim, J. F. Stoddart and O. K. Farha, *Science*, 2020, **368**, 297.

48 E. Masika and R. Mokaya, *Energy Environ. Sci.*, 2014, **7**, 427.

49 P. Pfeifer, L. Aston, M. Banks, S. Barker, J. Burress, S. Carter, J. Coleman, S. Crockett, C. Faulhaber, J. Flavin, M. Gordon, L. Hardcastle, Z. Kallenborn, M. Kemiki, C. Lapilli, J. Pobst, R. Schott, P. Shah, S. Spellerberg, G. Suppes, D. Taylor, A. Tekeei, C. Wexler, M. Wood, P. Buckley, T. Breier, J. Downing, S. Eastman, P. Freeze, S. Graham, S. Grinter, A. Howard, J. Martinez, D. Radke, T. Vassalli and J. Ilavsky, *Chaos*, 2007, **17**, 041108.

50 J. Romanos, S. Sweany, T. Rash, L. Firlej, B. Kuchta, J. C. Idrobo and P. Pfeifer, *Adsorpt. Sci. Technol.*, 2014, **32**, 681.

51 D. A. Gómez-Gualdrón, C. E. Wilmer, O. K. Farha, J. T. Hupp and R. Q. Snurr, *J. Phys. Chem. C*, 2014, **118**, 6941.

52 C. M. Simon, J. Kim, D. A. Gomez-Gualdron, J. S. Camp, Y. G. Chung, R. L. Martin, R. Mercado, M. W. Deem, D. Gunter, M. Haranczyk, D. S. Sholl, R. Q. Snurr and B. Smit, *Energy Environ. Sci.*, 2015, **8**, 1190.

53 M. E. Casco, M. Martínez-Escandell, K. Kaneko, J. Silvestre-Albero and F. Rodríguez-Reinoso, *Carbon*, 2015, **93**, 11.

54 S. Choi, M. A. Alkhabbaz, Y. Wang, R. M. Othman and M. Choi, *Carbon*, 2019, **141**, 143.

55 P. N. Quirant, C. Cuadrado-Collados, A. J. Romero-Anaya, J. S. Albero and M. M. Escandell, *Ind. Eng. Chem. Res.*, 2020, **59**, 5775.

56 B. M. Connolly, M. Aragones-Anglada, J. Gandara-Loe, N. A. Danaf, D. C. Lamb, J. P. Mehta, D. Vulpe, S. Wuttke, J. Silvestre-Albero, P. Z. Moghadam, A. E. H. Wheatley and D. Fairen-Jimenez, *Nat. Commun.*, 2019, **10**, 2345.

57 B. M. Connolly, D. G. Madden, A. E. H. Wheatley and D. Fairen-Jimenez, *J. Am. Chem. Soc.*, 2020, **142**, 8541.

58 V. Rozyyev, D. Thirion, R. Ullah, J. Lee, M. Jung, H. Oh, M. Atilhan and C. T. Yavuz, *Nat. Energy*, 2019, **4**, 604.

59 J. Abdulsalam, J. Mulopo, S. O. Bada and B. Oboirien, *ACS Omega*, 2020, **5**, 32530.

60 S. Ma, D. Sun, J. M. Simmons, C. D. Collier, D. Yuan and H. C. Zhou, *J. Am. Chem. Soc.*, 2008, **130**, 1012.